*Supplemental Information for*

# Temporal Changes in Thirdhand Cigarette Smoke Film Composition and the Potential for Oxidation of Co-existing Surface Film Chemicals

April M. Hurlock and Douglas B. Collins

Department of Chemistry, Bucknell University, Lewisburg, PA, 17837

*Corresponding Author: Douglas B. Collins, dbc007@bucknell.edu

## Contents

## S1. Experimental Apparatus

Details of the setup are given in the main text, but a short supplemental description will be given here along with a schematic in Figure S1. Sidestream cigarette smoke was generated in an apparatus built in-house that was contained inside a fume hood. A research cigarette was mounted into a modified vacuum flange that was bored out to a dimension that would snugly fit a cigarette. Draw for the mainstream smoke was generated with a diaphragm pump; mainstream smoke was filtered and then exhausted into the back of the fume hood. The vacuum flange used as a cigarette holder was then mounted onto a KF25 vacuum tee fitting for smoke generation. Ultra-pure air (a.k.a. – zero air) was delivered to the side arm of the tee, and sidestream smoke was emitted to the glass experimental chamber through a brass ¼-inch tube stub mounted on the third opening in the tee. Smoke injection commenced for 2 minutes, at which time the 2-liter glass experimental chamber was sealed. Some smoke was emitted into the fume hood from the experimental chamber during injection. The time period of injection, the puffing protocol, and the sweep air flow rate were held consistent, but the amount of smoke in the chamber was not separately quantified or fully constrained. Discussion of the use of a chemical tracer for the amount of smoke deposited on the slides is provided below. The sample substrates were glass slides that were placed on top of a larger glass microscope slide used as a stage, shown in gray in Figure S1. The glass chamber and the glass stage were cleaned by soaking in a base bath (1 M sodium hydroxide in isopropanol) after each experiment, then rinsed thoroughly with water and dried in an 100° C oven.

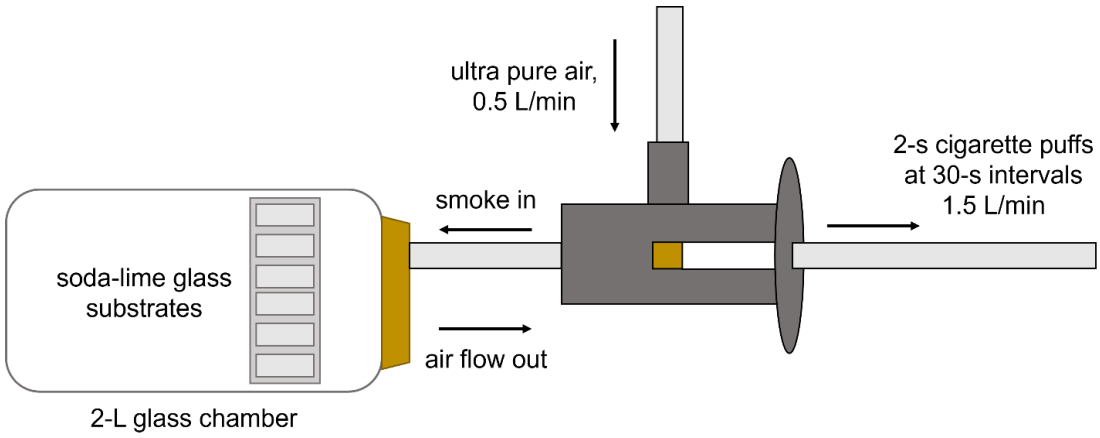


**Figure S1**: Schematic of the heart of the experimental apparatus for the generation of side-stream tobacco smoke and deposition on glass substrates.

## S2. Method Details for Liquid Chromatography/Mass Spectrometry Analysis

Methodological details for the analysis of thirdhand smoke (THS) components, beyond those given in the main text, are provided below.

### *S1.1 Liquid Chromatography (LC)*

Mobile phase gradients used for the present study, organized by analyte, are given in Table S1. Oxidation products of tris(2-carboxyethyl) phosphine (TCEP), oleic acid (OA), and squalene (SQ)

were identified using the same chromatographic method as their respective starting materials. Tobacco alkaloids, TCEP and TCEP oxide were measured using the same chromatographic method. Mobile phase reservoirs denoted in Table S1 were assigned to the following letter abbreviations:

A 0.1% formic acid in deionized water

B 100% acetonitrile

C 10% methanol in 10 mM ammonium formate, pH = 8.5

D 100% methanol

**Table S1**: LC-MS mobile phase gradients used for the analysis of specified analyte groups

| Analyte | Chromatographic Method |
|---|---|
| Tobacco Alkaloids<br>TCEP | 10% D and 90% C for 1 min, 10-95% D for 4 min, hold 95% D for 5 min, 5-90% C for 0.25 min; 3 min equilibrium time |
| OA | 5% A and 95% B for 5 min |
| SQ | 50% A and 50% B for 1 min, 50-100% B for 2 min, hold 100% B for 13 min, 0-50% A for 0.1 min; 4 min equilibrium time |

*S1.2 Mass Spectrometry (MS)*

Settings for the Agilent 6560 ion mobility quadrupole/time-of-flight (IM-Q-ToF) mass spectrometer for experiments in electrospray ionization (ESI) and atmospheric pressure chemical ionization (APCI) modes are given in Table S2. The instrument was operated in Q-ToF only mode (ion mobility separations were disabled) throughout the present study. Different settings were used for ESI in positive and negative ion modes. Negative ion mode was only used for OA and OA oxidation product analysis. APCI was only used in positive ion mode and restricted to the analysis of SQ and its oxidation products.

**Table S2**: Settings used for the Agilent 6560 Q-ToF mass spectrometer

*ESI Mode*

| Method ID | ESI+ | ESI- |
|---|---|---|
| Analyte(s) | Tobacco Alkaloids, TCEP | OA |
| Acquisition Range (m/z) | 50-1700 | 50-1700 |
| Acquisition Rate (spectra/s) | 10 | 10 |
| Polarity | + | - |
| Gas Temp (°C) | 325 | 325 |
| Drying Gas (L/min) | 13 | 13 |
| Nebulizer (psi) | 35 | 20 |
| Sheath Gas Temp (°C) | 275 | 300 |
| Sheath Gas Flow (L/min) | 11 | 10 |
| Capillary Voltage (V) | 4000 | 4000 |
| Nozzle Voltage (V) | 0 | 0 |
| Fragmentor Voltage (V) | 400 | 400 |

*APCI Mode*

| Method | APCI+ |
|---|---|
| Analyte(s) | SQ |
| Acquisition Range (m/z) | 50-1700 |
| Acquisition Rate (spectra/s) | 5 |
| Polarity | + |
| Gas Temp (°C) | 325 |
| Vaporizer (°C) | 500 |
| Drying Gas (L/min) | 8 |
| Nebulizer (psi) | 35 |
| Capillary Voltage (V) | 1900 |
| Corona+ (µA) | 4 |
| Fragmentor Voltage (V) | 400 |

Tandem mass spectrometry (MS/MS) was used for compound identification purposes. MS/MS was only conducted on tobacco alkaloids and SQ, so only method details for positive ion mode ESI and APCI are given in Table S3. Precursor m/z 152.0706 corresponded with the internal standard (acetaminophen).

**Table S3**: MS/MS settings and target lists for fragmentation

**ESI+**

| Analyte(s) | | Tobacco Alkaloids |
|---|---|---|
| Acquisition Range (m/z) | | 50-1700 |
| Acquisition Rate (spectra/s) | | 5 |
| *Target List* | | |
| Precursor Mass (m/z) | Iso Width | Collision Energy (eV) |
| 152.0706 | Narrow (~1.3 m/z) | 20 |
| 163.1230 | Narrow (~1.3 m/z) | 20 |
| 177.1026 | Narrow (~1.3 m/z) | 20 |
| 179.1181 | Narrow (~1.3 m/z) | 20 |
| 234.1031 | Narrow (~1.3 m/z) | 30 |

**APCI+**

| Analyte(s) | | SQ + oxidation products |
|---|---|---|
| Acquisition Range (m/z) | | 30-1700 |
| Acquisition Rate (spectra/s) | | 3 |
| *Target List* | | |
| Precursor Mass (m/z) | Iso Width | Collision Energy (eV) |
| 425.3766 | Narrow (~1.3 m/z) | 20 |
| 427.3928 | Narrow (~1.3 m/z) | 15 |

## S3. Suspect Screening of THS Film Extracts

A suspect-screening analysis was performed on the THS extracts from clean glass using MS1 data. The identifier in the 'Label' column correspond with Figure 1 in the main text. Mass accuracy may also be called the mass measurement error[1] and was calculated using Equation S1, where $m_i$ was the measured mass-to-charge ratio and $m_p$ was the predicted mass-to-charge ratio based on the associated molecular formula. Predicted masses were generated using ChemCalc.[2]

$$Mass\ Accuracy = \frac{m_i - m_p}{m_i} \times 10^6 \qquad [S1]$$

**Table S4**: Detected tobacco alkaloid compounds in a THS film deposited on clean glass

| Measured m/z $[M+H]^+$ | RT (min) | Label | Putative Match(es) | Predicted Neutral Formula | Predicted m/z $[M+H]^+$ | Mass Accuracy (ppm) |
|---|---|---|---|---|---|---|
| 147.0922 | 5.44 | mz147 | Myosmine | $C_9H_{10}N_2$ | 147.0922 | 0.0 |
| 149.1079 | 4.14 | mz149 | Nornicotine | $C_9H_{12}N_2$ | 149.1073 | 4.0 |
| 157.0766 | 5.76 | mz157 | 2,3'-bipyridine | $C_{10}H_8N_2$ | 157.0760 | 3.8 |
| 161.1079 | 6.22 | mz161 | N-methylmyosmine, anabasine, anatabine | $C_{10}H_{12}N_2$ | 161.1073 | 3.7 |
| 163.1231 | 5.95 | mz163 | Nicotine | $C_{10}H_{14}N_2$ | 163.1230 | 0.6 |
| 177.1026 | 4.15 | mz177a | Cotinine | $C_{10}H_{12}N_2O_2$ | 177.1022 | 2.3 |
| | 4.37 | mz177b | N-formylnornicotine | | | |
| 179.1181 | 1.96 | mz179a | Nicotine 1'-N-oxides | $C_{10}H_{14}N_2O$ | 179.1179 | 1.1 |
| | 2.10 | mz179b | | | | |
| 193.0501 | 4.41 | mz193 | Scopoletin | $C_{10}H_8O_4$ | 193.0495 | 3.1 |
| 234.1031 | 6.30 | mz234 | Nicotelline | $C_{15}H_{11}N_3$ | 234.1026 | 2.1 |
| 240.1501 | 6.90 | mz240 | Anatalline | $C_{15}H_{17}N_3$ | 240.1495 | 2.5 |

## S4. Identification of Selected Tobacco Alkaloids

A selection of alkaloids found in tobacco smoke were identified using liquid chromatography coupled to quadrupole/time-of-flight mass spectrometry (LC-Q-ToF MS). An overlay of MS1 extracted ion chromatograms corresponding to key tobacco alkaloid analytes extracted from clean glass after 170 h incubation are shown in Figure S2. Tandem MS spectra (Figure S3) were obtained for the tobacco alkaloids to aid in compound identification, especially for the isomers at m/z 177.1026. Tandem MS analysis of the nicotine oxide isomers at m/z 179.1181 is presented in Figure S4. MS/MS data for the nicotine oxide peaks are highly similar, indicating that the isomers are most likely nicotine 1'-N-oxide diastereomers. The MS/MS data for nicotine, nicotelline, cotinine, N-formylnornicotine, and nicotine 1'-N-oxide were compared against authentic standards.

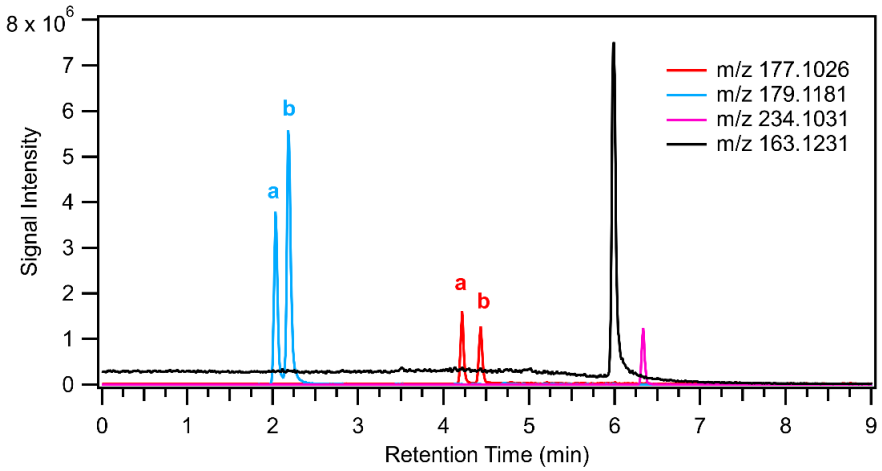


**Figure S2**: Overlay of extracted ion chromatograms (EICs) for four key mass-to-charge ratios used for relative quantification across various cases in the present study. The two EICs having two peaks each contain "a" and "b" labels that correspond with Table S4, where the putative identifications of a variety of detected compounds can be found. MS/MS spectra for each chromatographic peak shown in this figure can be found in Figures S3 and S4.

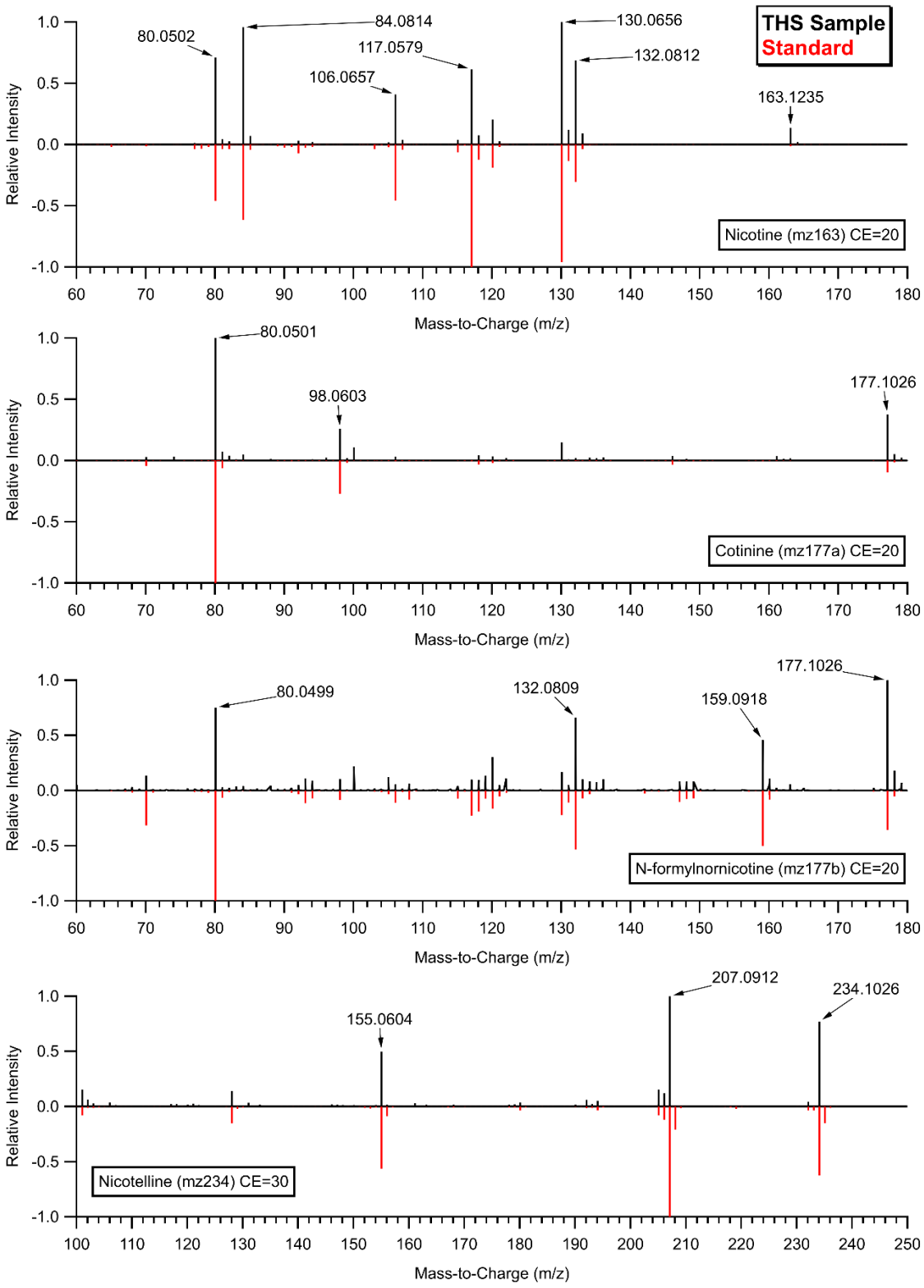


**Figure S3**: MS/MS data collected for each of the chromatographic peaks shown in Figure S2. Collision energy (CE) has been labeled in each panel. The red data was collected from standards.

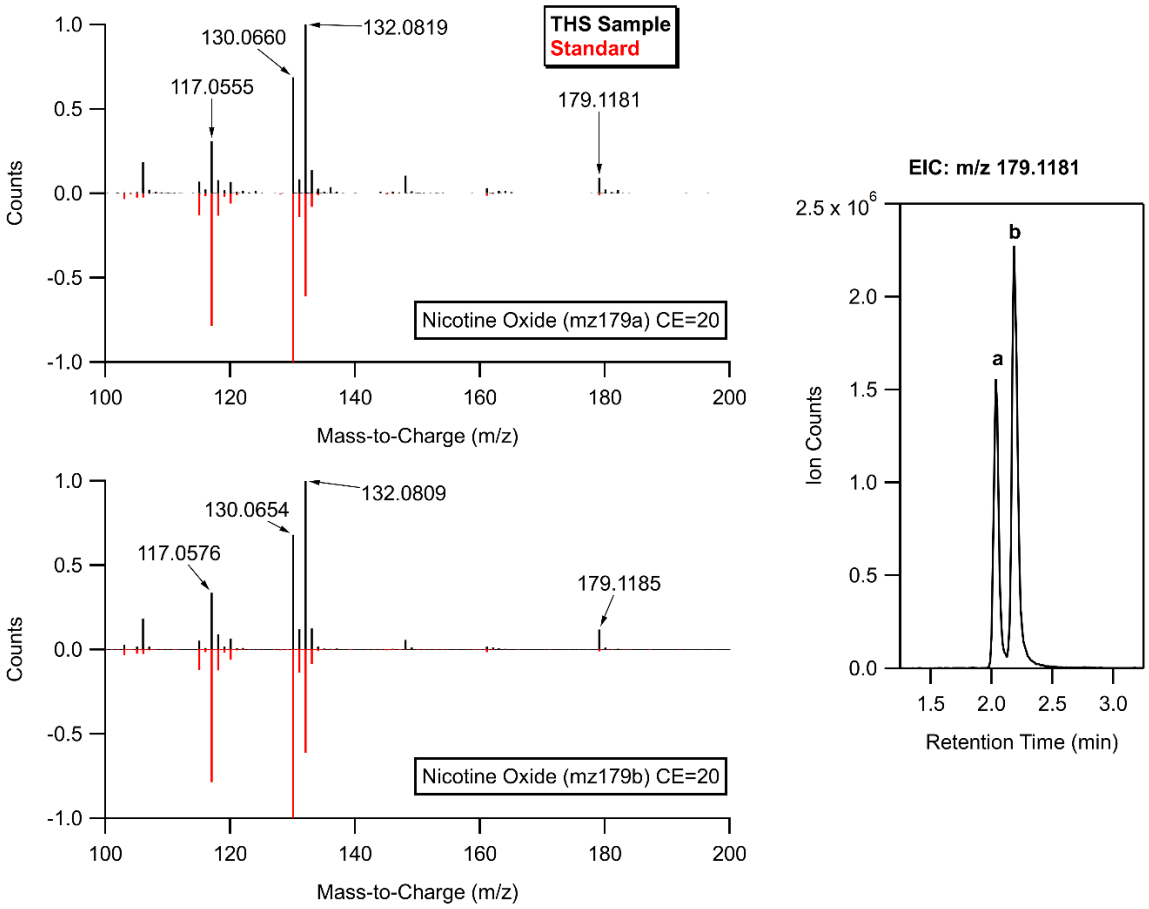


**Figure S4**: LC-MS/MS measurements of nicotine 1'-N-oxide diastereomers. (A) and (B) show collision-induced dissociation MS2 spectra for the precursor at m/z 179.1181, corresponding with each chromatographic peak. Note the high degree of spectral similarity. Panel (C) shows the extracted ion chromatogram for m/z 179.1181.

## S5. Replicate Clean Glass THS Incubation Experiments

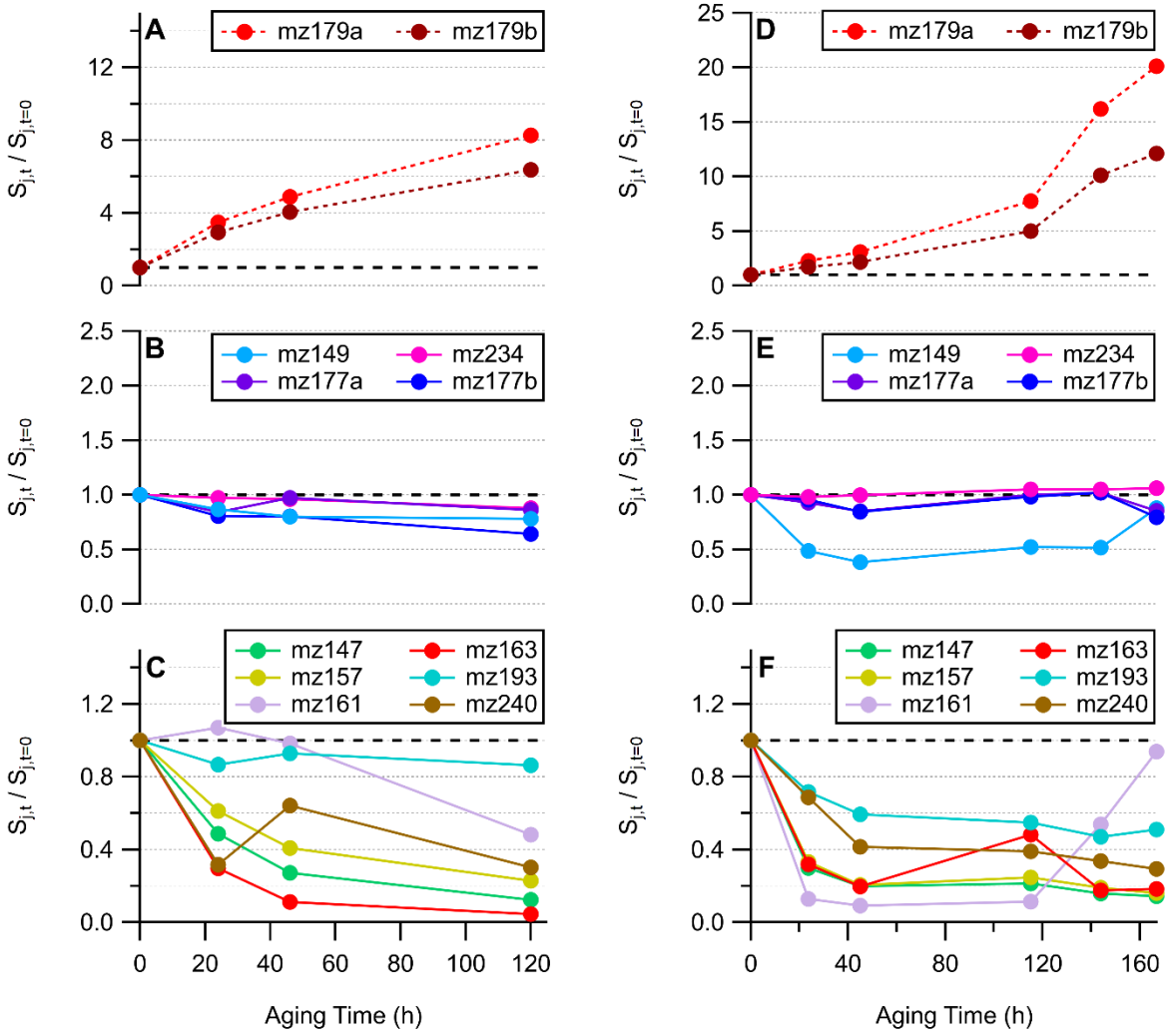


**Figure S5**: Replicate results for THS incubation on clean glass. Data in panels A-C were collected in a single experiment (Expt G2) and data in panels D-F were collected in another experiment (Expt G3). The format is intended to mirror the format of Figure 1 in the main text. Experiment labeling given in this caption corresponds with labeling in Figures S6 and S7.

## S6. The Potential Use of Nicotelline as a Tracer for Smoke Deposition Quantity

Nicotelline has been suggested as a conserved tracer species for tobacco smoke in the environment,[3,4] and has been used in the present study to ensure that THS films were generated uniformly across all sample substrates in a particular experiment. Inspection of nicotelline across experiments may allow for a means to normalize or adjust the measurements for differences in smoke generation and/or deposition. In order to explore information that may be contained within the nicotelline data, measurements have been compiled across six experiments (two sets of triplicate experiments; Figure S6). The black bar shows the average of the red bars with propagated uncertainty. Internal standard-normalized nicotelline signal was somewhat consistent across

experiments (average 0.09±0.05; relative standard deviation 55%; median 0.09). The variability in nicotelline suggests the scale of variation in smoke introduction across the six experiments shown in this demonstration. Inspecting one set of triplicate samples (THS on clean glass) in greater detail, the signals for key nicotine alkaloids were normalized to nicotelline at each time point in each experiment, and then is juxtaposed with the method shown in the main text – normalization to the first sample collected in each experiment (Figure S7). Normalizing the data to nicotelline did not indicate much improved compensation for experiment-to-experiment variations, and the main thesis of the study is retained within both normalization procedures. Normalizing to the first sample in each experiment has the benefit of indicating a 'fold-change' metric that is conceptually useful.

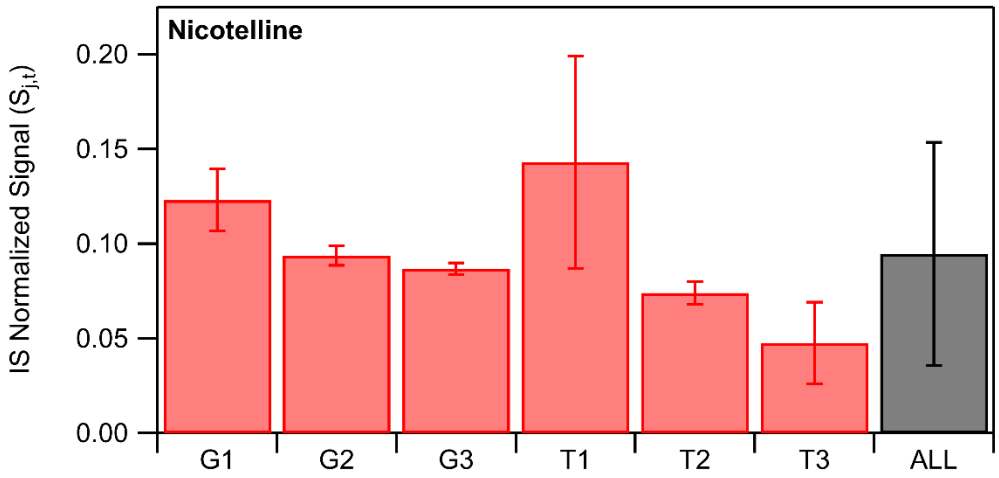


**Figure S6**: Internal standard-normalized signal for nicotelline averaged over all substrates in each clean glass (G1, G2, G3) and TCEP-coated glass (T1, T2, T3) experimental replicate. Error bars indicate the standard deviation of nicotelline signal values from each sample substrate within each experiment. The average of the red bars is represented in the black bar with propagated uncertainty. Experiment G1 is shown in Figure 1 of the main text, and experiment T1 is shown in Figures 2 and 3.

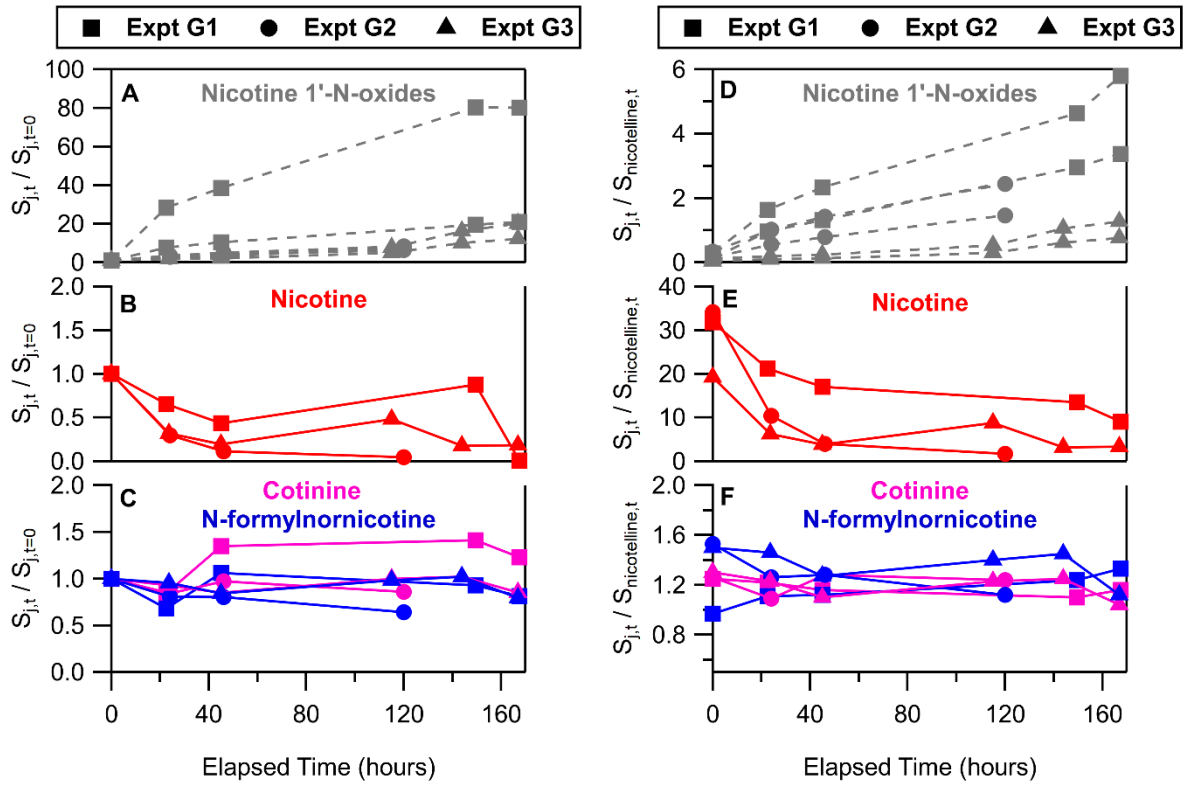


**Figure S7**: Overlay of key tobacco alkaloids in extracts from THS incubation experiments on clean glass. Data from three different experiments are compiled and are distinguished by marker shape. Data in panels A-C were normalized to the first sample in each experiment ($S_{j,t} / S_{j,t=0}$) while data in panels D-F were normalized to the corresponding nicotelline signal ($S_{j,t} / S_{nicotelline,t}$).

## S7. Control Experiments for Tris(2-carboxyethyl)phosphine as a Deposited Oxidant Probe

Tris(2-carboxyethyl)phosphine (TCEP) was used to detect oxidation in deposited THS films. Phosphines such as TCEP and triphenylphosphine are commonly used as reducing agents and/or antioxidants in chemical and biochemical laboratories. TCEP is a notable candidate for a surface film oxidation probe since it has a low volatility and a well-described oxide product, in which oxygen adds to the central phosphorus atom. TCEP can be oxidized rapidly in water in the presence of $O_2$, but control experiments (Figure S8) demonstrate that oxidation of a solid film of TCEP does not proceed over a 100 hour time period. Some background TCEP oxide was commonly detected in control samples and was commonly present in the TCEP stock solution to some degree but was accounted for through normalization of the time series data to the initial time point and reporting relative changes during incubation.

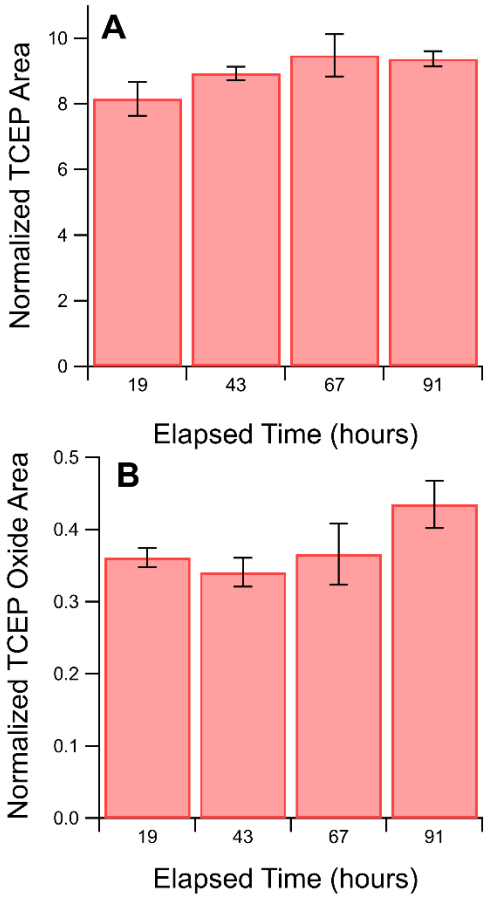


**Figure S8**: Internal standard normalized peak areas for TCEP and TCEP oxide incubated as dry films on soda-lime glass under zero air.

## S8. Replicate Incubations of THS on TCEP

Measurements of key chemical species from replicate incubations of THS films on TCEP-coated glass are shown in Figure S9. The general temporal trends for nicotine, nicotine 1'-N-oxides, TCEP, and TCEP oxide each behaved similarly across the three replicate trials (Figure S9 A and B), demonstrating that the overall oxidative effect observed in the present study was consistently observed in the experiments. The outcomes of the THS+TCEP experiment occupied a range of values; the differences between trials was the largest in the measurement of TCEP (Figure S9 C and D). We highlight that the experimental protocol did not provide much control over the quantity of smoke delivered to the sample substrates, which was addressed by normalizing the data to the first sample in each experiment. We note that the comparative magnitudes across compounds (e.g., TCEP vs nicotine) sometimes varied, so we maintain only moderate confidence about the numerical value of each species at a given time point.

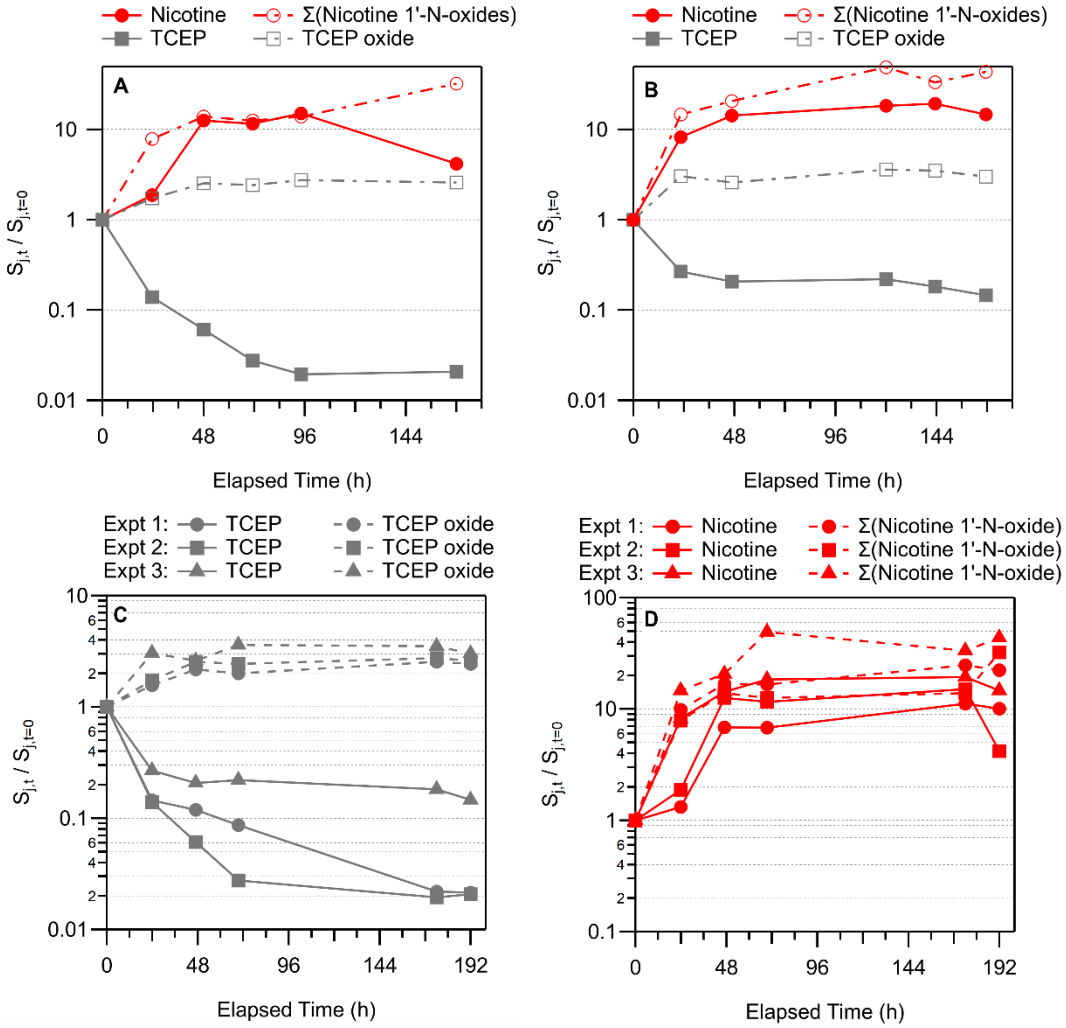


**Figure S9:** Replicate incubations of sidestream cigarette smoke residue on glass that was pre-coated with TCEP. The format of (A) and (B) was intended to mirror Figure 2 in the main text. Panels (C) and (D) are the same data, but plotted as overlays of all three replicate trials.

## S9. THS Deposition on Bis(2-ethylhexyl)sebacate (BES)

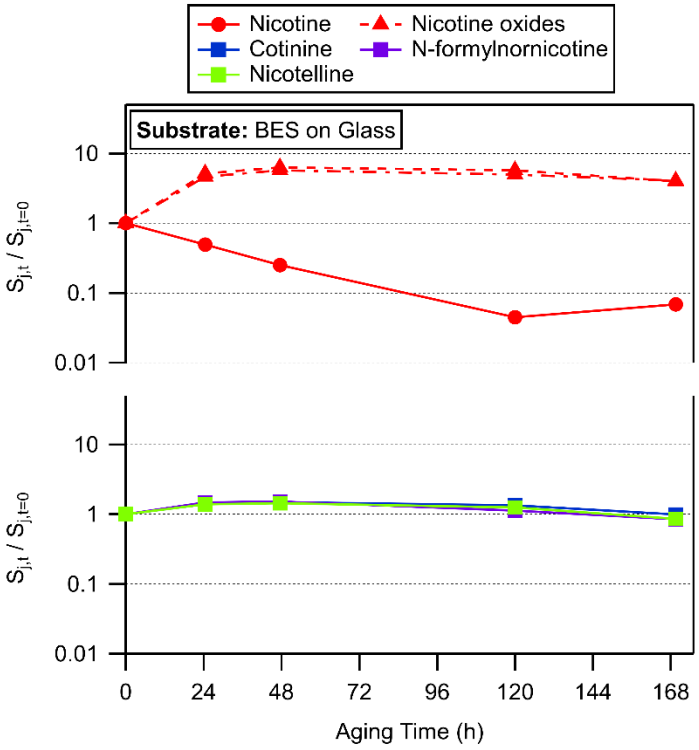


**Figure S10**: Temporal changes in key tobacco-related alkaloids upon cigarette smoke deposition to a BES film on glass.

## S10. Characterization of Oleic Acid Oxidation Products

**Table S5**: Chromatographic peaks in EICs from OA+THS experiments

| Measured m/z [M-H]- | RT (min) | Label in Fig. 5 | Predicted Formula | Predicted m/z [M-H]- | Mass Accuracy (ppm) |
|---|---|---|---|---|---|
| 297.2435 | 1.41 | 1 | $[C_{18}H_{34}O_3\text{-}H]^-$ | 297.2430 | 0.1 |
| | 1.61 | 2 | | | |
| | 1.78 | 3 | | | |
| 295.2276 | 1.35 | 4 | $[C_{18}H_{34}O_4\text{-}H_2O\text{-}H]^-$ | 295.2273 | 1.0 |
| | 1.44 | 5 | | | |
| 281.2488 | 2.35 | - | $[C_{18}H_{34}O_2\text{-}H]^-$ | 281.2481 | 0.6 |

A standard for epoxidated oleic acid (cis-9,10-epoxyoctadecanoic acid) was obtained and yielded a single chromatographic peak with retention time of 1.64 min, similar to Peak 2 (Figure S11).

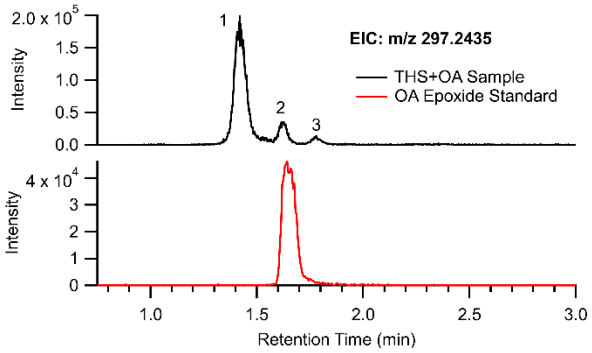


**Figure S11**: Comparison of the EIC for m/z 297.2435 from OA+THS data replicated from Figure 5 with the same EIC for an authentic cis-9,10-epoxyoctadecanoic acid (OA epoxide) standard.

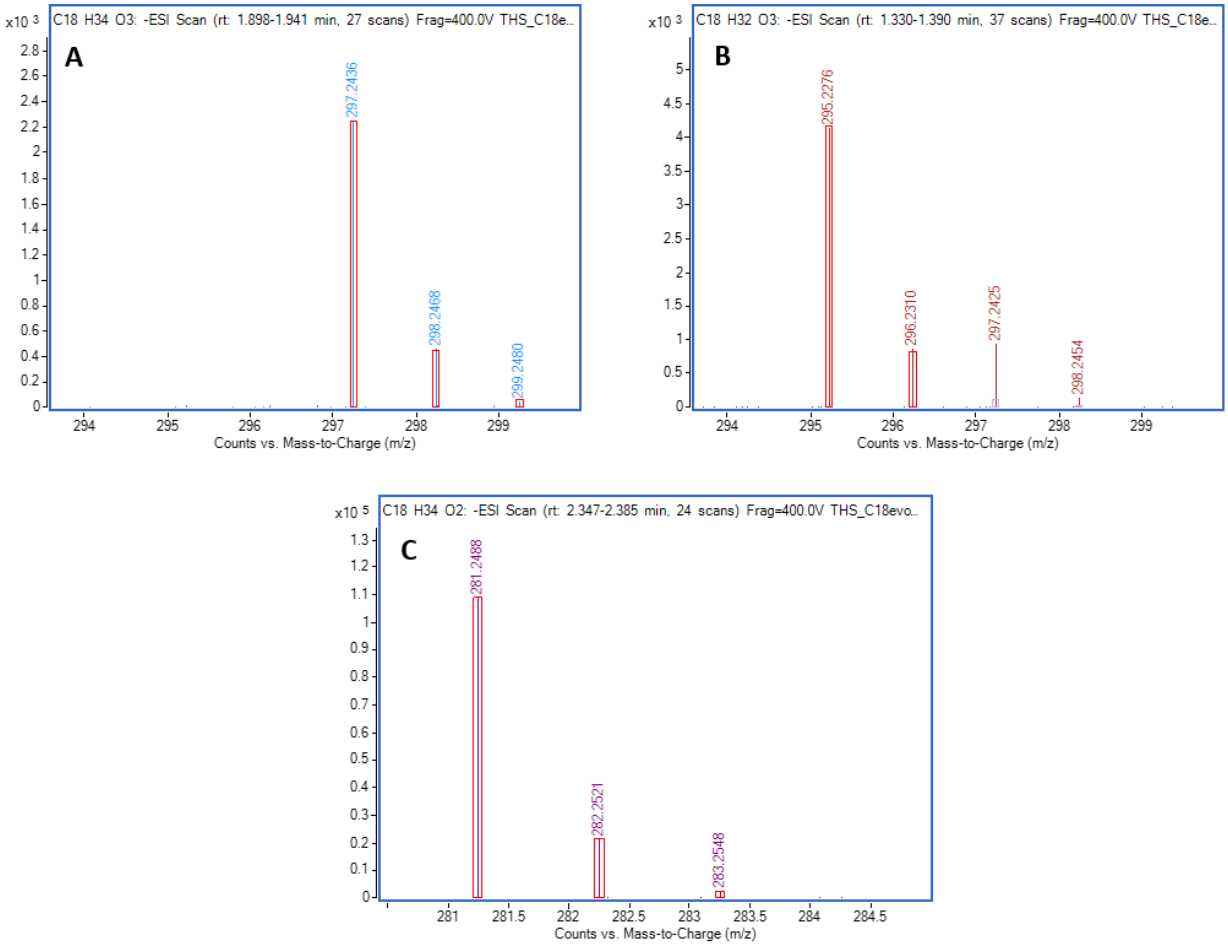


**Figure S12**: High resolution mass spectra for OA oxidation products (A and B), along with unreacted OA (C) in an OA+THS sample after 600 hours of incubation. Red boxes indicate the predicted stable isotope ratios based on the neutral molecular formula given in the upper left corner of each panel (ionized as $[M-H]^-$). Note that the species in (B) with the most abundant ion at m/z 425.2276 is labeled with a neutral molecular formula of $C_{18}H_{32}O_3$, which is equivalent to $C_{18}H_{34}O_4$ after loss of $H_2O$.

## S11. OA/BES Exposure to Zero Air

Sample substrates prepared with an OA/BES coating were incubated under zero air for up to 161 hours, and oxidation product formation was monitored using the same analytical method as the THS treatments. The three chromatographic peaks observed for OA+O (m/z 297.2435) showed little-to-no formation during the first ~100 hours of the incubation, the period in which most of the change was observed in the THS+OA study (Figure S13). The areas of all OA+O peaks in samples collected up to 113 hours of zero air incubation were similar to those obtained when analyzing a control sample directly from the OA stock solution. All three OA+O species had increased under zero-air incubation in the final (161 h) sample collected. The areas of OA+O Peaks 2 and 3 increased more than Peak 1 during zero air incubation. In contrast, OA+O Peak 1 was consistently the largest of the three in the THS treatment, plus it had already become elevated in area by the time the t=0 sample was collected (which was actually held under smoke for 30 mins while dry deposition was allowed to occur).

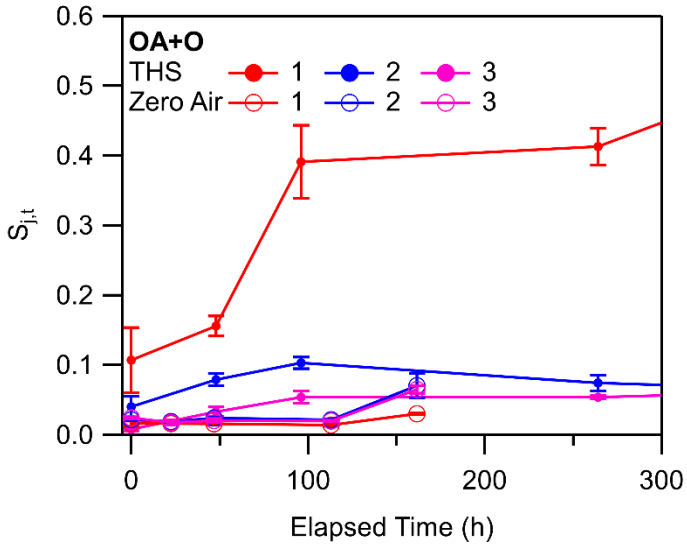


**Figure S13**: Comparison of the time series for the formation of OA+O species under THS incubation (solid circles, reproduced from Figure 5D) with incubation under zero air (open circles). Error bars show the standard deviation based on repeat LC-HRMS injections of each sample.

While two chromatographic peaks were clearly separable in the THS treatment, only one broad chromatographic peak was observed in the m/z 295.2276 extracted ion chromatogram during zero air incubation. Consequently, the broad peak was integrated as a single entity and the two separable peaks from the THS incubation were summed for a simple comparison. As shown in Figure S14, signal for OA+2O increased steadily during incubation with both zero air and THS. Therefore, we will not consider it further when specifically interpreting the THS-induced changes to film composition.

**Figure S14**: Comparison of the time series for the formation of OA+2O species under THS incubation (solid circles) with incubation under zero air (open circles). Error bars show the standard deviation with respect to repeated LC-HRMS injections.

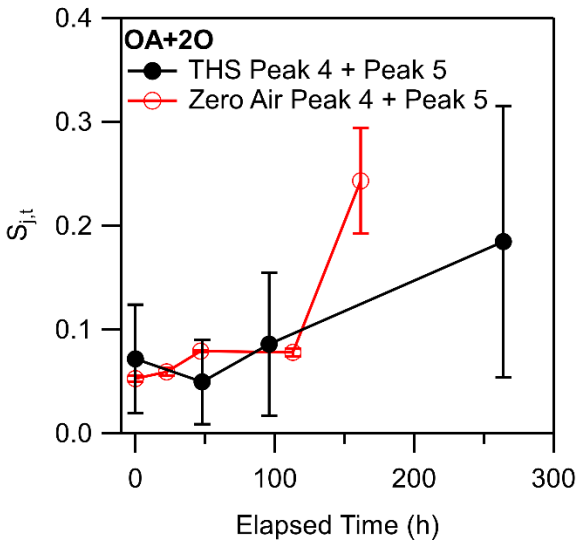


## S12. Characterization of Squalene Oxidation Products

**Table S6**: Chromatographic peaks in EICs from SQ+THS experiments

| Measured m/z [M-H]- | RT (min) | Label in Fig. 6 | Predicted Formula | Predicted m/z [M-H]- | Mass Accuracy (ppm) |
|---|---|---|---|---|---|
| 427.3944 | 9.05 | 1 | $[C_{30}H_{50}O+H]^+$ | 427.3940 | 2.0 |
| 425.3785 | 6.63 | 2 | $[C_{30}H_{50}O_2-H_2O+H]^+$ | 425.3783 | 1.5 |
| | 7.65 | 3 | | | |
| | 8.52 | 4 | | | |
| 411.3995 | 12.35 | - | $[C_{30}H_{50}+H]^+$ | 411.3991 | 2.2 |

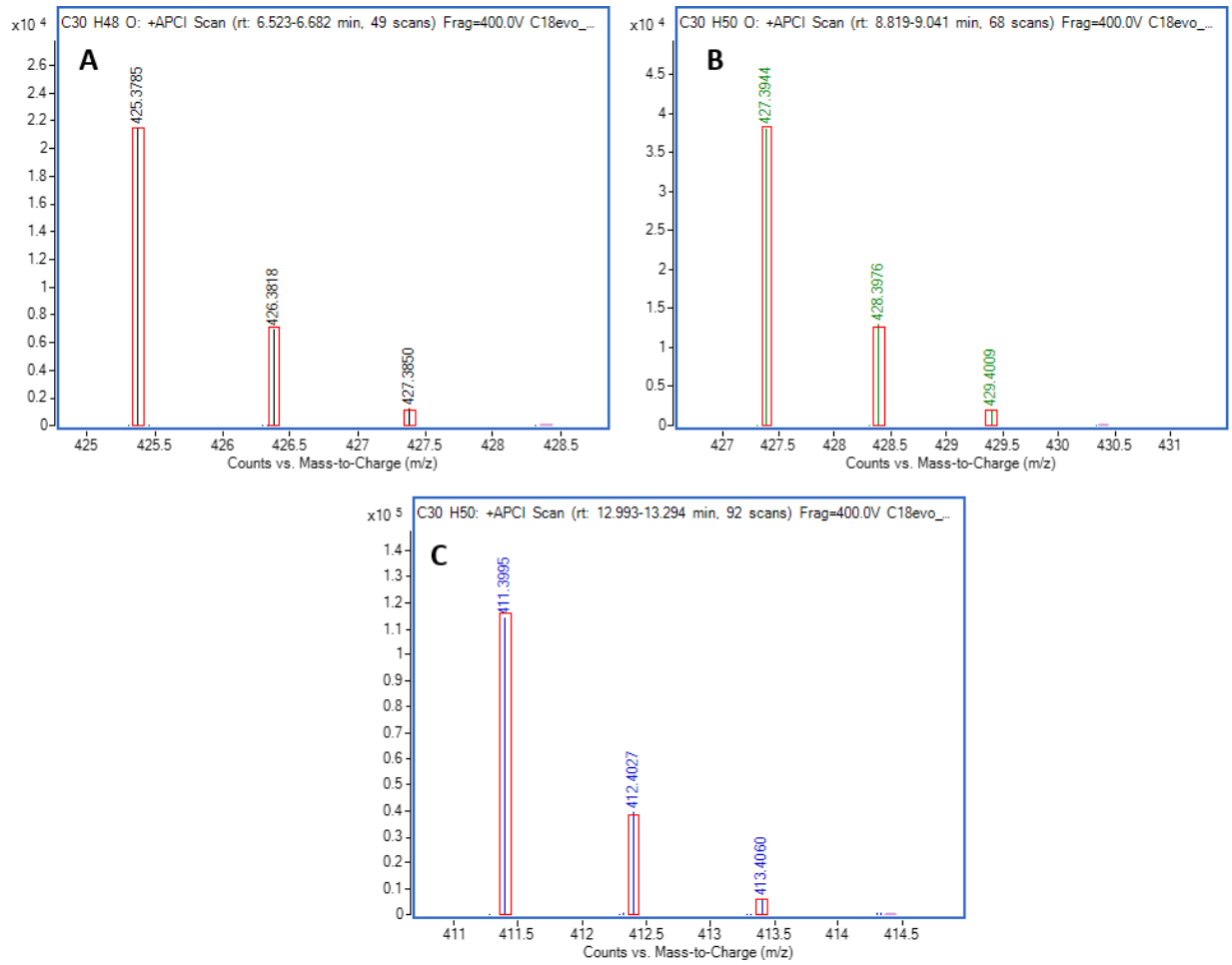


**Figure S15**: High resolution mass spectra for SQ oxidation products (A and B), along with unreacted SQ (C) in an SQ+THS sample after 216 hours of incubation. Red boxes indicate the predicted stable isotope ratios based on the neutral molecular formula given in the upper left corner of each panel (ionized as $[M+H]^+$). Note that the species in (A) with the most abundant ion at m/z 425.2276 is labeled with a neutral molecular formula of $C_{30}H_{48}O$, which is equivalent to $C_{30}H_{50}O_2$ after loss of $H_2O$.

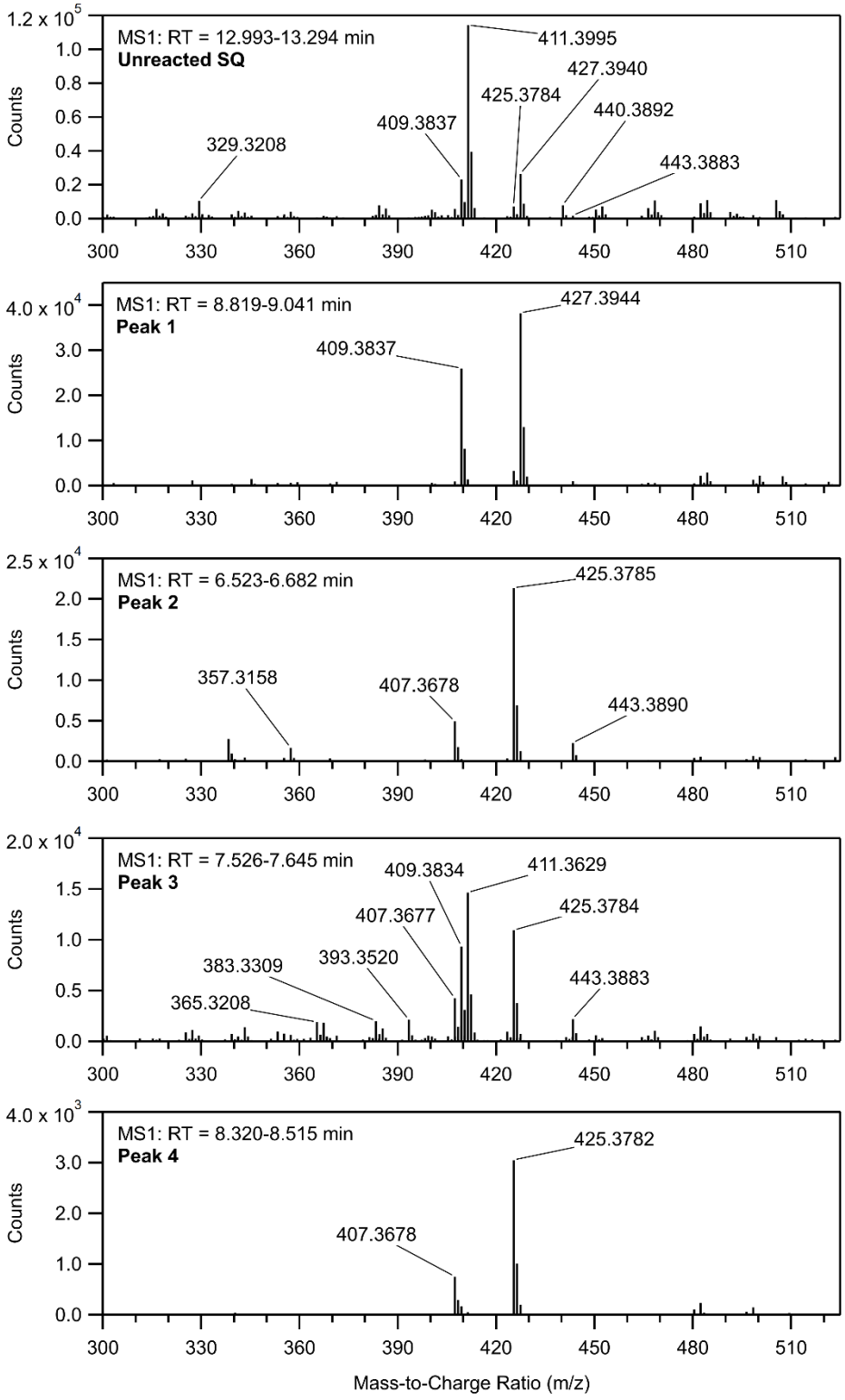


**Figure S16**: High resolution MS1 spectra corresponding to SQ and the four labeled chromatographic peaks for SQ oxidation products in Figure 6 of the main text. Retention time (RT) corresponds to the range of MS1 acquisition times used to generate each spectrum.

**Table S7**: Summary of ions observed in MS1 spectra shown in Figure S7

| Measured m/z | Found in Peak # | Predicted Ion Species Formula[2] | Calculated m/z | Mass Accuracy (ppm) |
|---|---|---|---|---|
| 329.3208 | SQ | $[C_{24}H_{40}+H]^+$ | 329.3208 | 0.08 |
| 357.3158 | 2 | $[C_{25}H_{40}O+H]^+$ | 357.3157 | 0.17 |
| 365.3208 | 3 | $[C_{27}H_{40}+H]^+$ | 365.3208 | 0.07 |
| 383.3309 | 3 | $[C_{27}H_{42}O+H]^+$ | 383.3314 | 1.28 |
| 393.3520 | 3 | $[C_{30}H_{50}O_2\text{-}H_2O\text{-}CH_3OH+H]^+$ | 393.3521 | 0.32 |
| 407.3678 | 2, 3, 4 | $[C_{30}H_{50}O_2\text{-}2H_2O+H]^+$ | 407.3678 | 0.06 |
| 409.3837 | SQ, 1<br>3 | $[C_{30}H_{50}O\text{-}H_2O+H]^+$<br>$[C_{30}H_{50}O_2\text{-}H_2O_2+H]^+$ | 409.3834 | 0.67 |
| 411.3629 | 3 | $[C_{30}H_{50}O_2\text{-}CH_3OH+H]^+$ | 411.3627 | 0.51 |
| 411.3995 | SQ | $[C_{30}H_{50}+H]^+$ | 411.3991 | 1.03 |
| 425.3782 | SQ, 2, 3, 4 | $[C_{30}H_{50}O_2\text{-}H_2O+H]^+$ | 425.3783 | 0.33 |
| 427.3944 | 1 | $[C_{30}H_{50}O+H]^+$ | 427.3940 | 0.96 |
| 443.3883 | SQ, 2, 3 | $[C_{30}H_{50}O_2+H]^+$ | 443.3889 | 1.37 |

Figure S16shows signals observed in the MS1 spectra collected during the elution of each peak labeled in Figure 6 of the main text. The salient m/z peaks are also tabulated in Table S7 with their annotated ion species. Peak 1 was characterized by prominent signals at m/z 427.3944 $[C_{30}H_{50}O+H]^+$ and m/z 409.3837 $[C_{30}H_{50}O\text{-}H_2O+H]^+$, suggesting the presence of squalene monoepoxide. Peaks 2, 3, and 4 each show prominent signals for m/z 425.3782 $[C_{30}H_{50}O_2\text{-}H_2O+H]^+$ and 407.3678 $[C_{30}H_{50}O_2\text{-}2H_2O+H]^+$, suggesting the in-source fragmentation of one or two $H_2O$ molecules from the SQ+2O precursor. Chromatographic peaks 2 and 3 were more intense than peak 4 and also include the intact SQ+2O precursor at m/z 443.3883 $[C_{30}H_{50}O_2+H]^+$. The prominence of m/z 425.3782 and m/z 407.3678 may be indicative of SQ-OOH species. Prior studies have sought to provide generalizable characteristics for SQ-OOH isomers with hydroperoxide substitution at tertiary vs secondary carbon atoms. While many ions observed in the present study were observed in prior studies, the MS1 and MS2 spectra in Figures S8 and S9 do not have consistent unique features in the same way as described in SQ photo-sensitized oxidation studies.[5,6] The MS1 spectrum for peak 3 showed many more signals than peaks 2 and 4. Signals corresponding to the in-source neutral loss of $CH_3OH$ (m/z 411.3629), along with the combined loss of $CH_3OH$ and $H_2O$ together (m/z 393.3520) were observed. In an MS1 spectrum for peak 3 that otherwise indicates a SQ+2O compound, the ion species assignment for m/z 409.3834 (Figure S16, Table S7) could be $[C_{30}H_{50}O_2\text{-}H_2O_2+H]^+$, consistent with a hydroperoxide molecular ion.

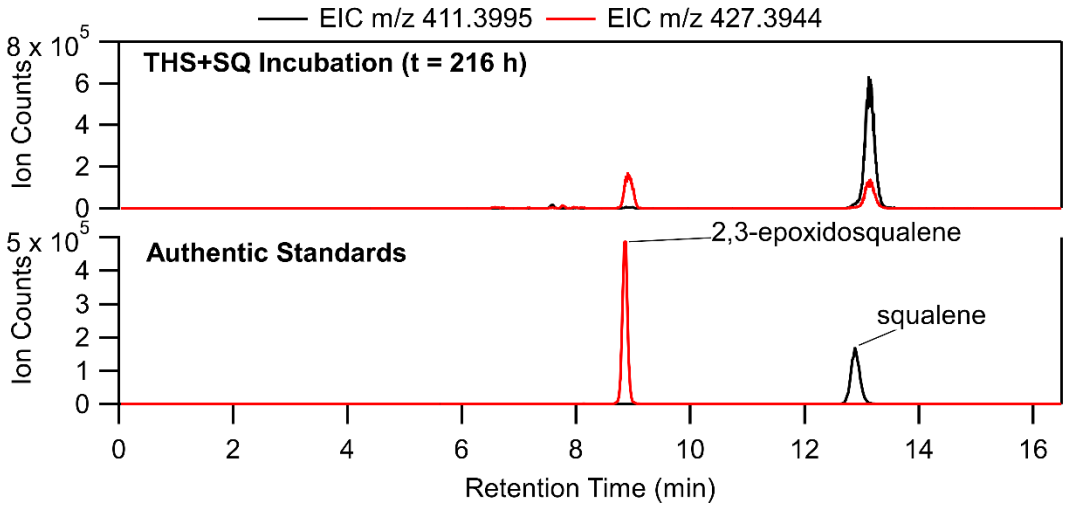


**Figure S17**: Comparison EICs from a THS+SQ sample with those from authentic standards of SQ epoxide and SQ. The standards were analyzed in separate LC-HRMS injections and are overlayed in the figure. Retention times of the standards closely match those of the THS+SQ sample.

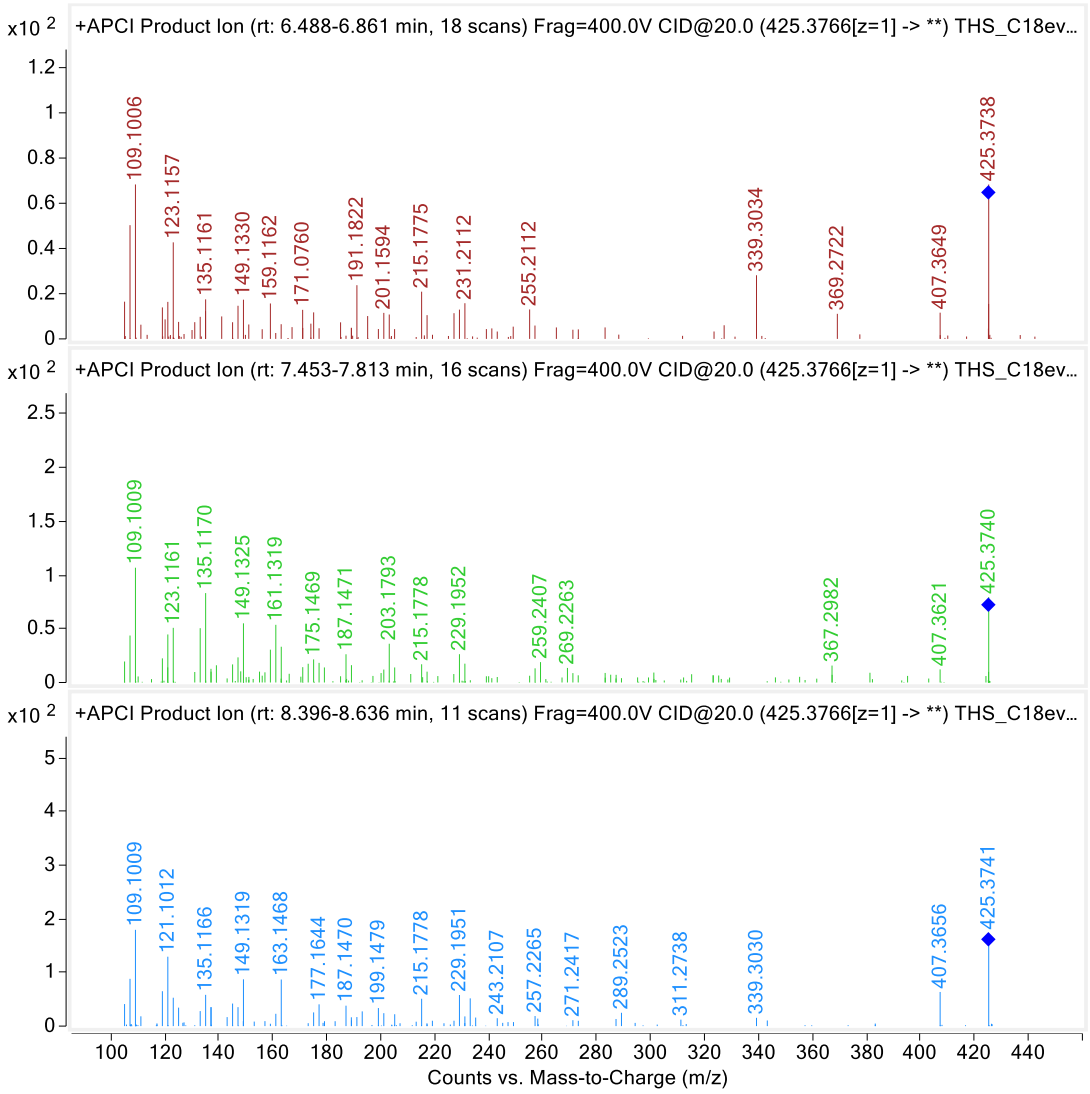


**Figure S18**: Tandem MS spectra for the three chromatographic SQ+2O peaks shown in Table S6 and Figure 6.

## S13. Exposure of Squalene to Zero Air

Samples prepared with SQ films were incubated under zero air for up to 161 hours. A comparison of SQ+O and SQ+2O signals from incubation under zero air with the same signals from THS incubation are depicted in Figure S19. Areas of SQ+2O peaks have been summed for simplicity, especially since their low abundance in the zero air incubation samples rendered poorer chromatographic resolution and signal-to-noise ratio. The presence of a signal corresponding to SQ+O was observed in the SQ stock solution and decayed over time on the film up to 113 h, before increasing again at 161 h. The signal for SQ+2O increased over time during incubation under zero air, but to a degree that was negligible in comparison to the THS case, so it appears not to vary in Figure S19. Incubation of SQ with THS appears to introduce substantial changes to SQ films due to oxidation.

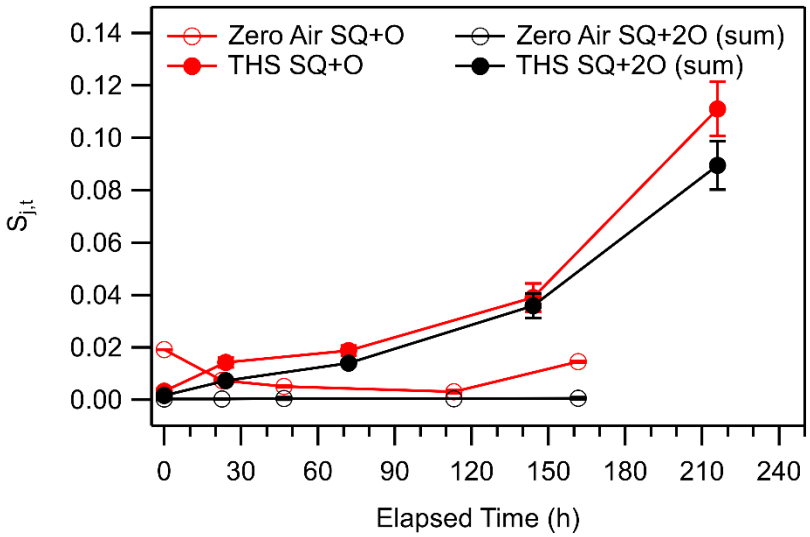


**Figure S19**: Comparison of the time series for SQ+O and SQ+2O species when incubated with THS (solid circles) and under zero air (open circles). Error bars have been applied to all four data traces and represent the standard deviation across repeated LC-HRMS injections.

## References

1 A. G. Brenton and A. R. Godfrey, *J. Am. Soc. Mass Spectrom.*, 2010, **21**, 1821–1835.
2 L. Patiny and A. Borel, *J. Chem. Inf. Model.*, 2013, **53**, 1223–1228.
3 P. Jacob, M. L. Goniewicz, C. M. Havel, S. F. Schick and N. L. Benowitz, *Chem. Res. Toxicol.*, 2013, **26**, 1615–1631.
4 N. J. Aquilina, C. M. Havel, P. Cheung, R. M. Harrison, K.-F. Ho, N. L. Benowitz and P. Jacob III, *Environment International*, 2021, **150**, 106417.
5 N. Shimizu, H. Bersabe, J. Ito, S. Kato, R. Towada, T. Eitsuka, S. Kuwahara, T. Miyazawa and K. Nakagawa, *J. Oleo Sci.*, 2017, **66**, 227–234.
6 K. Nakagawa, D. Ibusuki, Y. Suzuki, S. Yamashita, O. Higuchi, S. Oikawa and T. Miyazawa, *Journal of Lipid Research*, 2007, **48**, 2779–2787.